Immune Netw. 2023 Dec;23(6):e46
https://doi.org/10.4110/in.2023.23.e46
pISSN 1598-2629·eISSN 2092-6685

IMMUNE NETWORK

Original Article

IL-17 Imbalance Promotes the Pyroptosis in Immune-Mediated Liver Injury Through STAT3-IFI16 Axis

Wenfang Xu [1,*,†], **Yanan Wang** [1,†], **Changzhong Jin** [2], **Weiyang Zhang** [1], **Jiangnan Chen** [1], **Xuefang Chen** [1], **Junli Gao** [3,4], **Junshun Gao** [3,4], **Hong Wang** [3,4,*]

[1]Department of Clinical Laboratory, Affiliated Hospital of Shaoxing University, Shaoxing 312020, China
[2]State Key Laboratory for Diagnosis and Treatment of Infectious Diseases, Zhejiang University, Hangzhou 310027, China
[3]Hangzhou Cosmos Wisdom Mass Spectrometry Center of Zhejiang University Medical School, Hangzhou 311200, China
[4]Key Laboratory of Precision Medicine in Diagnosis and Monitoring Research of Zhejiang Province, Hangzhou 310016, China

Received: Aug 3, 2023
Revised: Nov 22, 2023
Accepted: Dec 6, 2023
Published online: Dec 11, 2023

***Correspondence to**
Wenfang Xu
Department of Clinical Laboratory, Affiliated Hospital of Shaoxing University, 999 Zhongxing South Road, Yuecheng District, Shaoxing 312020, China.
Email: 0052019050@usx.edu.cn

Hong Wang
Hangzhou Cosmos Wisdom Mass Spectrometry Center of Zhejiang University Medical School, 198 Qidi Road, Xiaoshan District, Hangzhou 311200, China.
Email: wh@cwmda.com

[†]Wenfang Xu and Yanan Wang contributed equally to this work.

ORCID iDs
Wenfang Xu
https://orcid.org/0009-0000-4909-4667
Yanan Wang
https://orcid.org/0000-0002-9936-049X
Changzhong Jin
https://orcid.org/0000-0001-6329-1739
Weiyang Zhang
https://orcid.org/0009-0007-3161-336X

ABSTRACT

Autoimmune hepatitis (AIH) affects all age group and occurs mainly in women. Pyroptosis is a novel programmed cell death featured with cell bursting and release of proinflammatory cytokines. A deeper understanding of AIH pathogenesis will contribute to novel therapy for AIH patients. Here, we aimed to investigate the role of IL-17 in immune-mediated liver injury. The levels of cytokines were measured by ELISA, and mRNA levels of STAT3 and IFN gamma-inducible protein 16 (IFI16) were detected by PCR. Expressions of STAT3, IFI16, gasdermin D and cleaved caspase-1 were measured by western-blotting. Immunohistochemical staining and transmission electron microscopy were applied to evaluate liver histopathological changes of the treated mice. Our results showed that the levels of IFI16 was increased in hepatocytes treated with IL-17 protein, and further elevated after STAT3-overexpressed (STAT3-OE) lentivirus treatment. The levels of IFI16 were reduced in hepatocytes treated with IL-17 neutralizing Ab (nAb), but were significantly increased after STAT3-OE treatment. Pyroptosis was observed in hepatocytes treated with IL-17 protein, and further cell damage was observed after STAT3-OE lentivirus treatment. Liver damage was alleviated in mice treated with IL-17 nAb, however sever damage was experienced after STAT3-OE lentivirus treatment. A binding interaction between IFI16 and STAT3 was detected in IL-17 treated hepatocytes. Glutathione transaminase activity was enhanced in concanavalin A-induced AIH mice compared to the control group ($p<0.01$). IL-17 plays an important role in activating STAT3 and up-regulating IFI16, which may promote the pyroptosis in AIH-related liver injury through STAT3-IFI16 axis.

Keywords: Autoimmune hepatitis; IL-17; Pyroptosis; IL-17-STAT3-IFI16 axis; Liver injury

INTRODUCTION

Autoimmune hepatitis (AIH) occurs mainly in women and contributes to various liver diseases (1-4). AIH is an inflammation disease due to the loss of immunological tolerance to hepatocytes, which promotes the progression of liver damage and excessive production of

Jiangnan Chen
https://orcid.org/0000-0002-1041-9927
Xuefang Chen
https://orcid.org/0000-0003-4468-4195
Junli Gao
https://orcid.org/0009-0005-8447-0097
Junshun Gao
https://orcid.org/0009-0001-8437-5023
Hong Wang
https://orcid.org/0000-0002-0382-9936

Conflict of Interest
The authors declare no potential conflicts of interest.

Abbreviations
AIH, autoimmune hepatitis; ConA, concanavalin A; CT, cycle threshold; GSDMD, gasdermin D; IFI16, IFN gamma-inducible protein 16; nAb, neutralizing; RT-qPCR, real-time quantitative PCR; RIPA, radio-immunoprecipitation assay; STAT3-OE, STAT3-overexpressed; TEM, transmission electron microscopy; TPBS, 0.05% Tween 20 in PBS.

Author Contributions
Conceptualization: Xu W, Gao J[2], Wang H; Data curation: Wang Y, Jin C, Zhang W, Chen J, Chen X; Formal analysis: Wang Y, Chen J; Investigation: Xu W, Wang Y, Wang H; Methodology: Wang Y, Jin C, Zhang W; Project administration: Zhang W, Chen J; Resources: Jin C, Gao J[1]; Software: Gao J[2]; Supervision: Xu W; Validation: Gao J[1]; Visualization: Jin C; Writing - original draft: Xu W, Wang H; Writing - review & editing: Xu W, Wang H.

Gao J[1], Junli Gao; Gao J[2], Junshun Gao.

cytokines (5-7). It is evaluated by serum transaminases levels, presence of autoantibodies, and evidence of interface hepatitis (8-11). Study on the pathogenesis of AIH may promote novel intervention for AIH patients. Proinflammatory cytokines such as IL-17, IL-1β, IL-18, TNF-α, and IFN-γ are key factors associated with AIH (12-18). Th17 cells mainly secrete IL-17 and play an important function in the host defense against infection and autoimmunity (19). IL-17, involving in stimulating hepatic inflammation and immune cell infiltration, acts as a regulator facilitating T-cell activation and inflammatory responses (20,21). It accelerates the production and release of proinflammatory cytokines, and promotes the activation of STAT3 pathway (22). Although IL-17/Th17 pathway plays an important role in regulating immune responses in AIH development, the mechanism of AIH progression still remains unclear. Several studies have reported that elevated plasma/serum levels of IL-17 was detected in AIH patients relative to healthy controls (23,24). A deeper understanding the role of IL-17 in AIH pathogenesis will have significant impact on developing novel therapies for AIH patients.

Pyroptosis is a programmed inflammatory cell death, resulting in release of intracellular pro-inflammatory cytokines and activation of a strong inflammatory response (24,25). It was found that IL-17 induces pyroptosis in osteoblasts through NOD-like receptor protein 3 inflammasome pathway (26). Other studies showed that STAT3 and IFN gamma-inducible protein 16 (IFI16) are involved in the initiation of the pathogenesis of autoimmune diseases such as sclerosis and lupus (27-29). IL-17 may contribute to the cell pyroptosis in AIH through promoting the binding interaction of activated STAT3 with IFI16, and the formation of inflammasome complexes. Although aberrant activation of STAT3 has been reported in autoimmune diseases (29), the mechanism of IL-17-STAT3-IFI16 axis in AIH is unclear. In present work, we developed a comprehensive study on the function of IL-17 in immune-mediated hepatocyte pyroptosis in AIH using the primary hepatocytes model and BALB/c mouse model. Our findings suggest that IL-17 plays a pivotal role in the progression of pyroptosis in AIH through IL-17-STAT3-IFI16 axis by activating STAT3 and up-regulating IFI16. Therapeutic potential of targeting IL-17-STAT3-IFI16 pathway for AIH patients deserve to be further studied.

MATERIALS AND METHODS

Animals

Male BALB/c mice were purchased from Shanghai SLAC Laboratory Animal Co. Ltd (License Key: SCXK 2017-0005; Certificate No: 20170005049224, Shanghai, China) and bred in our facility. Mice were housed in temperature-controlled environment (22°C–25°C) with a 12 h light-dark cycle and ad libitum access to food and water, following the standards set by the National Institutes of Health Guidelines for the Care and Use of Laboratory Animals. All experimental protocols were approved by the Institutional Animal Care and Use Committee of the Affiliated Hospital of Shaoxing University (protocol ID. 20-10-06 SU).

Mice aged 7 to 9 wks old were used in this study. Littermate WT mice were used as a control for the concanavalin A (ConA)-induced AIH experiment. Mice were randomly divided into nine groups for different treatments (**Table 1**). There were 6 mice in each group, and each mouse was treated through tail vein injection except for the lentivirus infection injected intraperitoneally. Mice were sacrificed at indicated time and blood from orbital sinus was collected. Serum was separated by centrifuging at 3,000 rpm for 10 min at 4°C and used for the detection of liver function (glutathione transaminase activity) and cytokine levels.

Table 1. Background characteristics of the study groups

Group	Characteristics
Primary mouse hepatocytes.	
Control (n=3)	No treatment
IL-17 protein (n=3)	IL-17 protein
NC (n=3)	IL-17 protein
STAT3-OE (n=3)	IL-17 protein, STAT3-OE lentivirus
si-NC (n=3)	IL-17 Protein, scrambled shRNA lentivirus
si-STAT3 (n=3)	IL-17 protein, si-STAT3 lentivirus
IL-17 nAbs (n=3)	IL-17 nAb
IL-17 nAbs+STAT3-OE (n=3)	IL-17 nAb, STAT3-OE lentivirus
Mice	
Control (n=6)	No treatment
Model (n=6)	ConA
IL-17 nAbs (n=6)	IL-17 nAb, ConA
NC (n=6)	ConA
si-NC (n=6)	Scrambled shRNA lentivirus, ConA
STAT3-OE (n=6)	STAT3-OE lentivirus, ConA
si-STAT3 (n=6)	si-STAT3 lentivirus, ConA
IL-17 nAbs+STAT3-OE+CoA (n=6)	IL-17 nAb, STAT3-OE lentivirus, ConA
STAT3-OE+CoA (n=6)	STAT3-OE lentivirus, ConA

Model or **NC** (n=6): mice were challenged with 15 mg/kg ConA (C2010, Sigma-Aldrich, St. Louis, MO, USA) to establish AIH.

Control (n=6): mice were received an equal amount of 0.9% normal saline (IN9000, Solarbio Life Sciences, Beijing, China).

IL-17 neutralizing Abs (nAbs) (n=6): mice were administrated with IL-17 nAb (1 μg/kg) (MAB421-SP, Bio-Techne, Minneapolis, MN, USA) 30 min before injected with 15 mg/kg ConA.

STAT3-OE (n=6): lentivirus with a short hairpin RNA (shRNA, Santa Cruz Biotechnology, Inc. Santa Cruz, CA, USA) up-regulated expression of STAT3 was given at 10^8 virus per mouse every day for 7 days before the mouse was injected with 15 mg/kg ConA.

si-STAT3 (n=6): lentivirus with a shRNA down-regulated expression of STAT3 was given at 10^8 virus per mouse every day for 7 days before the mouse was injected with 15 mg/kg ConA.

si-NC (n=6): lentivirus with a negative scrambled shRNA lentivirus unregulated expression of STAT3 was given at 10^8 virus per mouse every day for 7 days before the mouse was injected with 15 mg/kg ConA.

IL-17 nAbs+STAT3-OE+ConA (n=6): mice were administrated with IL-17 nAb (1 μg/kg) 30 min before were given with STAT3-OE for 7 days, then were injected with 15 mg/kg ConA.

STAT3-OE+ConA (n=6): mice were given with STAT3-OE for 7 days before were injected with 15 mg/kg ConA.

Primary mouse hepatocytes

Primary mouse hepatocytes were purchased from Liver Biotechnology Co. Ltd (Cat# LV-PMH002, Shenzhen, China). Hepatocyte cells were divided into eight groups for different treatments (**Table 1**). Each treatment was conducted in triplicate in 150 mm tissue culture dish

(Cat# FB0875714, Thermo Fisher Scientific, Waltham, MA, USA). Cells were cultured in RPMI-1640 media (Cat# 11875093, Thermo Fisher Scientific) supplemented with 10% FBS, 100 mg/ml streptomycin and 100 IU/ml penicillin in a humidified incubator with 5% CO_2 at 37°C.

Control (n=3): cells were cultured as described above.

IL-17 protein (n=3): cells were treated with 100 ng/ml of IL-17 recombinant protein (Cat# P01621, Solarbio Life Sciences) for 24 h.

NC (n=3): cells were treated with 100 ng/ml of IL-17 recombinant protein for 24 h.

STAT3-OE (n=3): cells were treated with 100 ng/ml of IL-17 recombinant protein for 24 h, followed by treatment with the short hairpin RNA lentivirus that up-regulated the expression of STAT3 for 48 h.

si-STAT3 (n=3): cells were treated with 100 ng/ml of IL-17 recombinant protein for 24 h, followed by treatment with the short hairpin RNA lentivirus that down-regulated the expression of STAT3 for 48 h.

si-NC (n=3): cells were treated with 100 ng/ml of IL-17 recombinant protein for 24 h, followed by treatment with negative scrambled shRNA lentivirus that unregulated the expression of STAT for 48 h.

IL-17 nAbs (n=3): cells were treated with IL-17 nAb (1 μg/dish) for 24 h.

IL-17 nAbs+STAT3-OE (n=3): cells were treated with IL-17 nAb (1 μg/dish) for 24 h, followed by treatment with lentivirus up-regulated STAT3 for 48 h.

mRNA expression assay

Total RNA was extracted with Trizol reagent (Cat# 15596018, Invitrogen, Carlsbad, CA, USA) following the manufacturer's instructions. A NanoDrop ND-2000 instrument (Thermo Fisher Scientific) was used to evaluate the quality of RNA samples. A 2 μg of total RNA was used in reverse transcription with Prime Script RT Reagent Kit (Cat# R222-01, Vazyme Biotech, Nanjing, China) according to the manufacturer's protocol.

Real-time quantitative PCR (RT-qPCR)

RT-qPCR was conducted using IO-RAD CFX Connect Real-Time System (Applied Biosystems, Foster City, CA, USA) with ChamQ SYBR Color qPCR Master Mix (Cat# Q411-02, Vazyme Biotech). The Primers were purchased from Sunny Biotech (Shanghai, China) as listed in **Table 2**. The mRNA expression levels of target genes were calculated by the comparative cycle

Table 2. Primers used in this study

Name	Primer sequence (5′-3′)	PCR product size
Actin (F)	AGAGGGAAATCGTGCGTGAC	189 bp
Actin (R)	CCAAGAAGGAAGGCTGGAAA	
STAT3 (F)	GACATTCCCAAGGAGGAGGC	89 bp
STAT3 (R)	TACGGGGCAGCACTACCT	
IFI16 (F)	GACAACCAAGAGCAATACACCA	86 bp
IFI16 (R)	ATCAGTTTGCCCAATCCAGAAT	

https://doi.org/10.4110/in.2023.23.e46

threshold (CT) method ($2^{-\Delta\Delta CT}$) using ACTB as internal control according to the formula: $2^{-\Delta\Delta CT}$ (STAT3/or IFI16: ΔCt=mRNACt−ACTBCt, ΔΔCT=ΔCt−average control ΔCt).

Western blot

The cell culture media were removed and hepatocyte cells were lysed with radioimmunoprecipitation assay (RIPA) buffer (Cat# 89900, Thermo Fisher Scientific) supplemented with protease inhibitor cocktail (Cat# 78440, Thermo Fisher Scientific). The detached cells were re-suspended in 500 μl of ice-cold RIPA buffer and transferred into a microcentrifuge tube. After rotation for 20 min at 4°C, lysates were centrifuged at 20,000×g for 20 min at 4°C to remove cell debris. The cleared supernatants were transferred into fresh tubes and protein concentrations were determined using BCA Protein Assay kit (Cat# 23227, Thermo Fisher Scientific).

An aliquot of 20 μg of protein was mixed with an equivalent volume of loading buffer (pH 7.4, containing β-mercaptoethanol) and boiled for 5 min before separated using the SDS-PAGE (8%–10% polyacrylamide). After electrophoresis, proteins were transferred onto polyvinylidene difluoride membranes (Millipore, Billerica, MA, USA) and blotted against primary Abs at 4°C overnight. Membranes were washed three times with 0.05% Tween 20 in PBS(TPBS, pH 7.4) and incubated with 5% nonfat milk to block the nonspecific binding sites. Abs against STAT3 (Cat# GTX104616, 1:1,000) was purchase from GeneTex (Irvine, CA, USA), and IFI16 (Cat# ab169788, 1:1,000) and internal control GAPDH (Cat# ab181602, 1:5,000) were purchase from Abcam (Waltham, MA, USA). After washing three times with TPBS, the secondary Ab (Cat# ab150077, 1:5,000, Abcam) conjugated with HRP was incubated with the membranes at room temperature for 1 h and washed 5 times with 1×TBST for 5 min each time. Protein bands were revealed by enhanced chemiluminescence imaging system (SageCreation Science, Beijing, China) with SuperSignal™ West Femto Maximum Sensitivity Substrate (Thermo Fisher Scientific).

Dual-luciferase reporter assay

The binding interaction between STAT3 and IFI16 were analyzed by dual-luciferase reporter assay. The plasmid of pcDNA3.1, STAT3-pcDNA3.1, Wt-IFI16-pGL3 and Mut-IFI16-pGL3 were transfected with ExFect 2000 reagent (Cat# T202-03, Vazyme Biotech). Each transfected group contained four multiple pores, and dual luciferase reporter assay kit (Cat# E1910, Promega, Madison, WI, USA) was used to detect the luciferase activity after transfection for 48 h in GloMax 20/20 Luminometer (E5311, Promega) following the manufacturer's instructions. Luciferase values were normalized to those of Renilla luciferase.

Detection of cytokines

Concentrations of IFI16, IL-17, IL-1β, and IL-18 in tissue or serum from mice were measured using ELISA kits (Jianglai Bio, Shanghai, China) following the manufacturer's instructions. Each sample was tested in triplicate using SpectraMax Plus 384 system (Molecular Devices, San Jose, CA, USA).

Analysis of LDH

The cell culture media were transferred into microcentrifuge tubes, and centrifuged at 3,000×g for 15 min at 4°C to remove cell debris. The cleared media were transferred into fresh tubes. LDH levels in media were measured using the LDH assay kit (Cat# BC0685, Solarbio Life Sciences) following the manufacturer's instructions. Each sample was tested in triplicate.

Assay of glutathione transaminase activity

Mice were anesthetized after ConA-induced AIH for 8 h. Blood from orbital sinus was collected into microcentrifuge tubes and kept at room temperature for 30 min, followed by standing on ice for 1 h. Serum was separated at 3,000×g for 10 min at 4°C and used for the measurement of glutathione transaminase activities using Hitachi 7600 Automatic Analyzer.

Histopathology assessments

Liver tissues from mice were fixed in 4% paraformaldehyde fixative solution. The tissue sections were stained with H&E and observed under a light microscopy. Liver injury was evaluated based on the inflammation of the portal area, lobule and fusion necrosis. The degree of hepatic pathological damage was scored using a double blind method.

Score-0: no pathological change.
Score-1: hepatocyte edema, inflammatory cell infiltration, spotty necrosis, no focal necrosis area.
Score-2: increased inflammatory cell infiltration, visible focal necrosis area.
Score-3: massive focal necrosis area, disorder of the liver tissue structure.

Transmission electron microscopy (TEM)

Liver tissue (<1 mm^3) were seeded in 6-well plates and sequentially treated with 2.5% glutaraldehyde, 1% osmium tetroxide, and increasing gradient of ethanol and acetone. The tissue was fixed, dehydrated and embedded with Spurr's resin. After slicing in the electron microscope UC6 ultramicrotome (Leica Microsystems, Wetzlar, Germany), the samples were adhered to uncoated copper grids and stained with 4% uranyl acetate. Then, the stained samples were observed under the transmission electron microscopy (TECNAI 10, Philips, Eindhoven, Netherlands).

Statistical analysis

Statistical analyses were performed using the statistical package GraphPad Prism version 8.0 (GraphPad Software, San Diego, CA, USA). All data were displayed as mean±SD for at least three independent experiments per each group. Statistical comparisons were made using one-way ANOVA or Student's *t*-test. A p-value <0.05 was considered statistically significant.

RESULTS

Effect of lentivirus-regulated STAT3 in mouse primary hepatocytes

Expression level of STAT3 was significantly up-regulated in cells treated with STAT3-OE lentivirus compared to that in NC group ($p<0.01$, STAT3-OE vs. NC), and down-regulated in cells treated with si-STAT3 lentivirus compared to that in si-NC group ($p<0.01$, si-STAT3 vs. si-NC). As shown in **Fig. 1A**, the results indicated that the effectiveness of lentivirus-regulated STAT3 in mouse primary hepatocytes.

Increased mRNA levels of IFI16 in mouse primary hepatocytes treated with IL-17 recombinant protein and STAT3-OE lentivirus

As shown in **Fig. 1B**, the mRNA level of IFI16 was significantly increased in mouse primary hepatocytes treated with IL-17 recombinant protein compared to that in control group without IL-17 recombinant protein treatment ($p<0.01$, IL-17 protein vs. control). The expression of IFI16 mRNA was further elevated in hepatocytes treated with STAT3-OE lentivirus, compared to that in NC group without lentivirus treatment ($p<0.01$, STAT3-OE vs. NC). In contrast, the

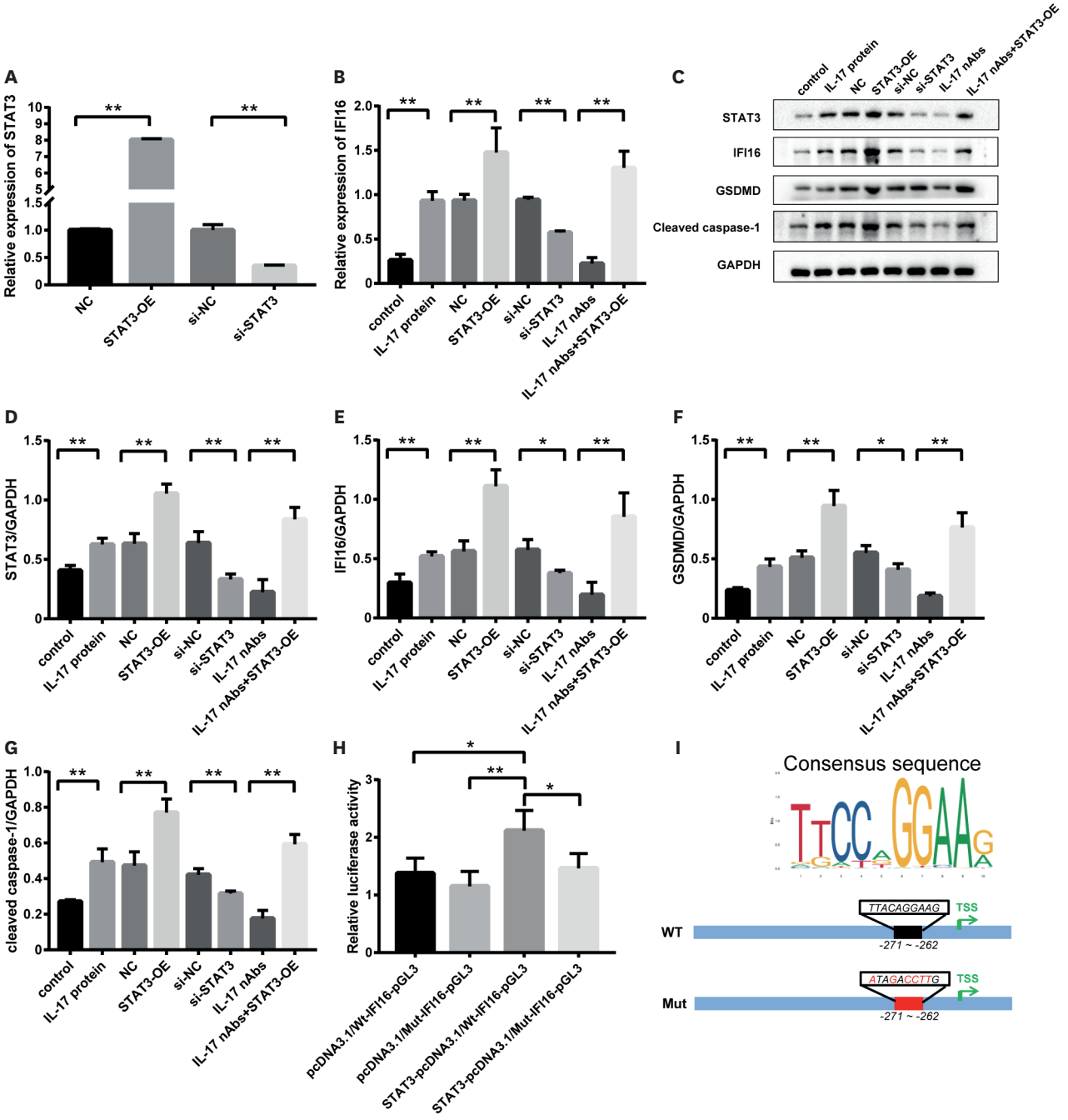

Figure 1. Primary mouse hepatocytes model and related assay. (A) Effect of lentivirus-mediated expression of STAT3. (B) IFI16 mRNA expression measured by PCR. (C) Western blot detection of STAT3, IFI16, GSDMD, cleaved caspase-1 and GAPDH. (D) STAT3 protein expression detected by Western blot. (E) IFI16 protein expression detected by Western blot. (F) GSDMD protein expression detected by Western blot. (G) cleaved caspase-1 protein expression detected by Western blot. (H) Interaction between STAT3 and IFI16 by dual-luciferase reporter assay. (I) Consensus sequence of binding sites between STAT3 and IFI16 (WT vs. Mut). Control (n=3), cells were cultured without treatment; NC (n=3), cells were treated with 100 ng/ml of IL-17 recombinant protein for 24 h; IL-17 protein (n=3), cells were treated with 100 ng/ml of IL-17 recombinant protein for 24 h; STAT3-OE (n=3), cells were treated with 100 ng/ml of IL-17 recombinant protein for 24 h, followed by treatment with the short hairpin RNA lentivirus that up-regulated the expression of STAT3 for 48 h; si-STAT3 (n=3), cells were treated with 100 ng/ml of IL-17 recombinant protein for 24 h, followed by treatment with the short hairpin RNA lentivirus that down-regulated the expression of STAT3 for 48 h; si-NC (n=3), cells were treated with 100 ng/ml of IL-17 recombinant protein for 24 h, followed by treatment with negative scrambled shRNA lentivirus that unregulated the expression of STAT for 48 h; IL-17 nAbs (n=3), cells were treated with IL-17 nAb (1 μg/dish) for 24 h; IL-17 nAbs+STAT3-OE (n=3), cells were treated with IL-17 nAb (1 μg/dish) for 24 h, followed by treatment with the short hairpin RNA lentivirus that up-regulated the expression of STAT3 for 48 h.
*p<0.05, **p<0.01.

https://doi.org/10.4110/in.2023.23.e46

mRNA level of IFI16 was significantly reduced in hepatocytes treated with si-STAT3 lentivirus compared to that in si-NC group treated with scrambled shRNA lentivirus ($p<0.01$, si-STAT3 vs. si-NC). The mRNA level of IFI16 was decreased in hepatocytes treated with IL-17 nAb, but was significantly elevated after STAT3-OE lentivirus treatment ($p<0.01$, IL-17 nAbs+STAT3-OE vs. IL-17 nAbs).

Increased protein levels of IFI16 and STAT3 in mouse primary hepatocytes treated with IL-17 recombinant protein and STAT3-OE lentivirus

As shown in **Fig. 1C-E**, the protein expression levels of IFI16 and STAT3 were significantly increased in IL-17 recombinant protein treated hepatocytes compared to that in control group without IL-17 recombinant protein treatment ($p<0.01$, IL-17 protein vs. control), and were further elevated in hepatocytes treated with STAT3-OE lentivirus compared to that in NC group without lentivirus treatment ($p<0.01$, STAT3-OE vs. NC). However, the protein expression levels of IFI16 and STAT3 were significantly decreased in hepatocytes treated with si-STAT3 lentivirus compared to that in si-NC group treated with scrambled shRNA lentivirus (STAT3: $p<0.01$, si-STAT3 vs. si-NC; IFI16: $p<0.05$, si-STAT3 vs. si-NC). Although the expression levels of IFI16 and STAT3 were reduced in hepatocytes treated with IL-17 nAb, their levels were significantly increased after STAT3-OE lentivirus treatment ($p<0.01$, IL-17 nAbs+STAT3-OE vs. IL-17 nAbs). Cell pyroptosis involved gasdermin D (GSDMD) and cleaved caspase-1 showed the similar expression changes as IFI16 and STAT3, as illustrated in **Fig. 1F** for GSDMD (all $p<0.01$, IL-17 protein vs. control, STAT3-OE vs. NC, IL-17 nAbs+STAT3-OE vs. IL-17 nAbs; $p<0.05$, si-STAT3 vs. si-NC) and **Fig. 1G** for cleaved caspase-1 (all $p<0.01$, IL-17 protein vs. control, STAT3-OE vs. NC, si-STAT3 vs. si-NC, IL-17 nAbs+STAT3-OE vs. IL-17 nAbs).

Binding interaction between STAT3 and IFI16

Dual-luciferase reporter assay showed that the ratio of luc/Rluc from the co-transfected Wt-IFI16 plasmid and STAT3-pcDNA3.1 plasmid is the highest among the other three paired groups (**Fig. 1H**), and the relative luciferase activity is statistically significant difference between STAT3-pcDNA3.1/Wt-IFI16-pGL3 and the other three paired groups. The consensus sequence and mutated sequences were illustrated in **Fig. 1I**.

$p<0.05$: STAT3-pcDNA3.1/Wt-IFI16-pGL3 vs. pcDNA3.1/Wt-IFI16-pGL3; $p<0.01$: STAT3-pcDNA3.1/Wt-IFI16-pGL3 vs. pcDNA3.1/Mut-IFI16-pGL3; $p<0.05$: STAT3-pcDNA3.1/Wt-IFI16-pGL3 vs. STAT3-pcDNA3.1/Mut-IFI16-pGL3.

Increased levels of cytokines in mouse primary hepatocytes treated with IL-17 recombinant protein and STAT3-OE lentivirus

ELISA assay of cytokines in culture medium showed that IFI16, IL-1β and IL-18 were significantly increased in hepatocytes treated with IL-17 recombinant protein, compared to that in control group without IL-17 recombinant protein treatment as shown in **Fig. 2A-C** (all cytokines $p<0.01$, IL-17 protein vs. control). The levels of above cytokines were further elevated in hepatocytes treated with STAT3-OE lentivirus compared to that in NC group without lentivirus treatment (all cytokines $p<0.01$, STAT3-OE vs. NC). In contrast, the expression levels of those cytokines were significantly decreased in hepatocytes treated with si-STAT3 lentivirus compared to that in si-NC group treated with scrambled shRNA lentivirus (all cytokines $p<0.01$, si-STAT3 vs. si-NC). Although above cytokine levels were reduced in hepatocytes treated with IL-17 nAb, their were significantly increased in hepatocytes treated with STAT3-OE lentivirus (all cytokines $p<0.01$, IL-17 nAbs+STAT3-OE vs. IL-17 nAbs).

https://doi.org/10.4110/in.2023.23.e46

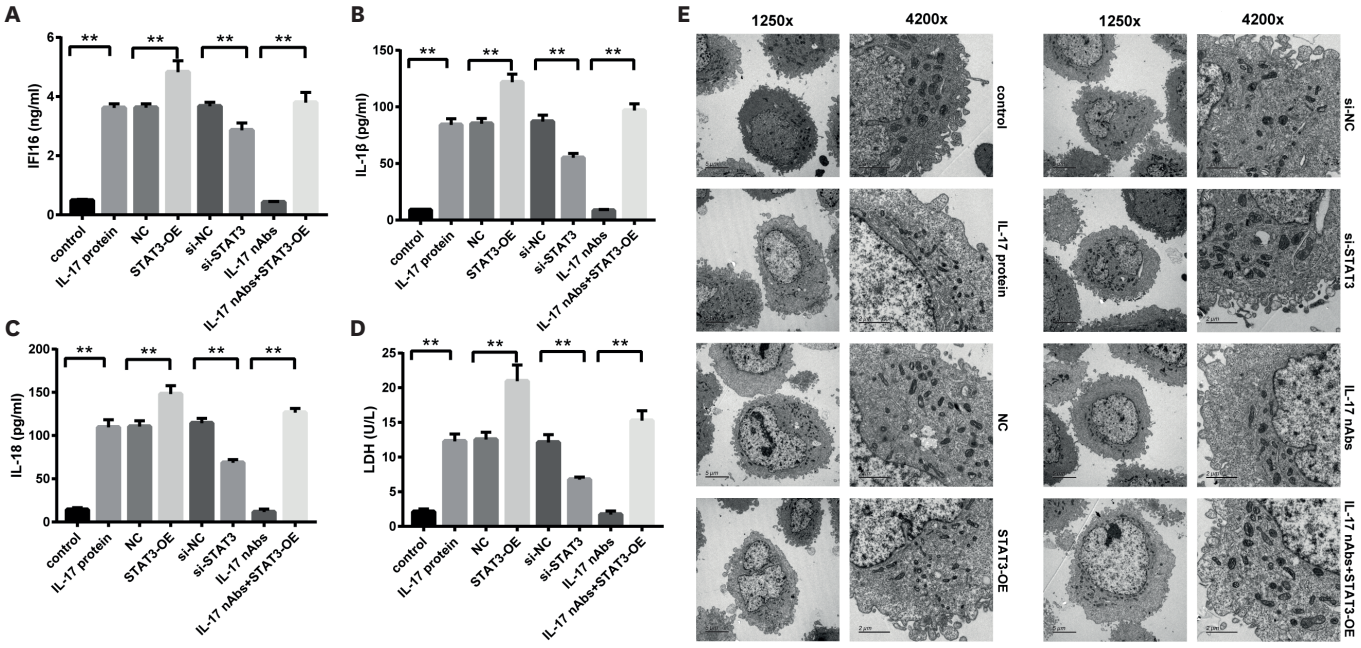

Figure 2. ELISA assay of cytokines in cell culture medium (A-D) and TEM observation of cell morphology changes. (A) IFI16, (B) IL-1β, (C) IL-18, (D) LDH, (E) Cell morphology and degree of cell damage.
Control (n=3), cells were cultured without treatment; NC (n=3), cells were treated with 100 ng/ml of IL-17 recombinant protein for 24 h; IL-17 protein (n=3), cells were treated with 100 ng/ml of IL-17 recombinant protein for 24 h; STAT3-OE (n=3), cells were treated with 100 ng/ml of IL-17 recombinant protein for 24 h, followed by treatment with the short hairpin RNA lentivirus that up-regulated the expression of STAT3 for 48 h; si-STAT3 (n=3), cells were treated with 100 ng/ml of IL-17 recombinant protein for 24 h, followed by treatment with the short hairpin RNA lentivirus that down-regulated the expression of STAT3 for 48 h; si-NC (n=3), cells were treated with 100 ng/ml of IL-17 recombinant protein for 24 h, followed by treatment with negative scrambled shRNA lentivirus that unregulated the expression of STAT for 48 h; IL-17 nAbs (n=3), cells were treated with IL-17 nAb (1 μg/dish) for 24 h; IL-17 nAbs+STAT3-OE (n=3), cells were treated with IL-17 nAb (1 μg/dish) for 24 h, followed by treatment with the shortcytokines hairpin RNA lentivirus that up-regulated the expression of STAT3 for 48 h.
**p<0.01.

Increased levels of LDH in mouse primary hepatocytes treated with IL-17 recombinant protein and STAT3-OE lentivirus

The level of LDH in culture medium was significantly increased in hepatocytes treated with IL-17 recombinant protein compared to that in control group without IL-17 recombinant protein treatment as shown in **Fig. 2D** (p<0.01, IL-17 protein vs. control). The level of LDH was further elevated in hepatocytes treated with STAT3-OE lentivirus compared to that in NC group without lentivirus treatment (p<0.01, STAT3-OE vs. NC). In contrast, the level of LDH was significantly reduced in hepatocytes treated with si-STAT3 lentivirus compared to that in si-NC group treated with scrambled shRNA lentivirus (p<0.01, si-STAT3 vs. si-NC). The level of LDH was reduced in hepatocytes treated with IL-17 nAb, but was significantly increased in hepatocytes treated with STAT3-OE lentivirus (p<0.01, IL-17 nAbs+STAT3-OE vs. IL-17 nAbs).

Observed pyroptosis in mouse primary hepatocytes treated with IL-17 recombinant protein and STAT3-OE lentivirus

The changes of cell morphology and degrees of cell damage in different conditions were observed by TEM (**Fig. 2E**). Compared to the control group, the hepatocytes treated with IL-17 recombinant protein appeared swelling, increased protrusion and vesicles, and deformed organelles. Severe cell damage occurred in hepatocytes treated with STAT3-OE lentivirus (i.e. STAT3-OE group) compared to that in NC group without STAT3-OE lentivirus treatment. The degree of cell damage became alleviated in hepatocytes treated with si-STAT3 lentivirus (i.e. si-STAT3 group) compared to that in si-NC group treated with scrambled shRNA lentivirus.

https://doi.org/10.4110/in.2023.23.e46

In addition, the degree of cell damage was alleviated in hepatocytes treated with IL-17 nAb, however severe cell damage was observed followed by STAT3-OE lentivirus treatment.

Elevated levels of cytokines in serum and tissue from mice treated with ConA and STAT3-OE lentivirus

The levels of cytokines (IFI16, IL-17, IL-1β, and IL-18) in both serum and liver tissue were significantly increased in ConA-induced AIH in mice (i.e. the model group) compared to that in control group without ConA treatment (all $p<0.01$, model vs. control) as shown in **Fig. 3A-D**. The levels of cytokines were further elevated in mice sequentially administrated with STAT3-OE lentivirus and ConA compared to that in NC group challenged with ConA only (STAT3-OE vs. NC: tissue IFI16 and IL-17, $p<0.05$; tissue IL-1β and IL-18, $p<0.01$; serum IFI16 and IL-17, $p<0.01$; serum IL-1β and IL-18, $p<0.05$). The levels of cytokines were significantly reduced in mice injected with si-STAT3 lentivirus compared to that in si-NC group injected with scrambled shRNA lentivirus (all $p<0.01$, si-STAT3 vs. si-NC). The ConA-induced liver damage was alleviated and levels of cytokines were remarkable reduced in mice administrated with IL-17 nAb (all $p<0.01$, IL-17 nAbs vs. model). In addition, the levels of cytokines were significantly reduced in mice treated sequentially with IL-17 nAb, STAT3-OE lentivirus and ConA compared to that in mice treated sequentially with STAT3-OE lentivirus and ConA (all $p<0.01$, IL-17 nAbs+STAT3-OE+ConA vs. STAT3-OE+ConA).

As showed in **Fig. 3A**, the comparison analysis between the group of "IL-17 nAb" and the group of "IL-17 nAb+STAT3-OE+ConA" indicated that there was significant difference in IFI16 levels between the group treated with "IL-17 nAb" and the group treated with "IL-17 nAb+STAT3-OE+ConA" (tissue: $p<0.05$; Serum: $p<0.01$). In addition, there were also significant differences between above two groups in the levels of other three cytokines including IL-17, IL-1β and IL-18 (tissue and serum, all $p<0.01$) as showed in **Fig. 3B-D**.

Increased glutathione transaminase activity in mice treated with ConA and STAT3-OE lentivirus

As shown in **Fig. 4A**, glutathione transaminase activities in serum were significantly increased in ConA-induced AIH mice (i.e. the model group) compared to that in control group without ConA treatment ($p<0.01$, model vs. control). There was no significant difference in glutathione transaminase activity between model group or NC group and si-NC group. However, glutathione transaminase activities were significantly increased in mice treated with STAT3-OE lentivirus and ConA compared to that in NC group treated with ConA only ($p<0.01$, STAT3-OE vs. NC). However, glutathione transaminase activities were significantly reduced in mice treated with si-STAT3 lentivirus compared to that in si-NC group treated with scrambled shRNA lentivirus ($p<0.01$, si-STAT3 vs. si-NC). Glutathione transaminase activities were significantly decreased in mice treated with IL-17 nAb 24 h before ConA injection compared to that in model group ($p<0.01$, IL-17 nAbs vs. model). Glutathione transaminase activities were also significantly reduced in mice treated sequentially with IL-17 nAb, STAT3-OE lentivirus and ConA compared to that in mice treated with STAT3-OE lentivirus and ConA (all $p<0.01$, IL-17 nAbs+STAT3-OE+ConA vs. STAT3-OE+ConA).

Histopathological changes in liver from mice treated with ConA, STAT3-OE lentivirus and IL-17 nAb

The liver pathology scores and histology changes from mice were observed under different treatments as shown in **Fig. 4B-C**. The pathology scores were significantly increased in ConA induced AIH mice (i.e. the model group) compared to that in control group without

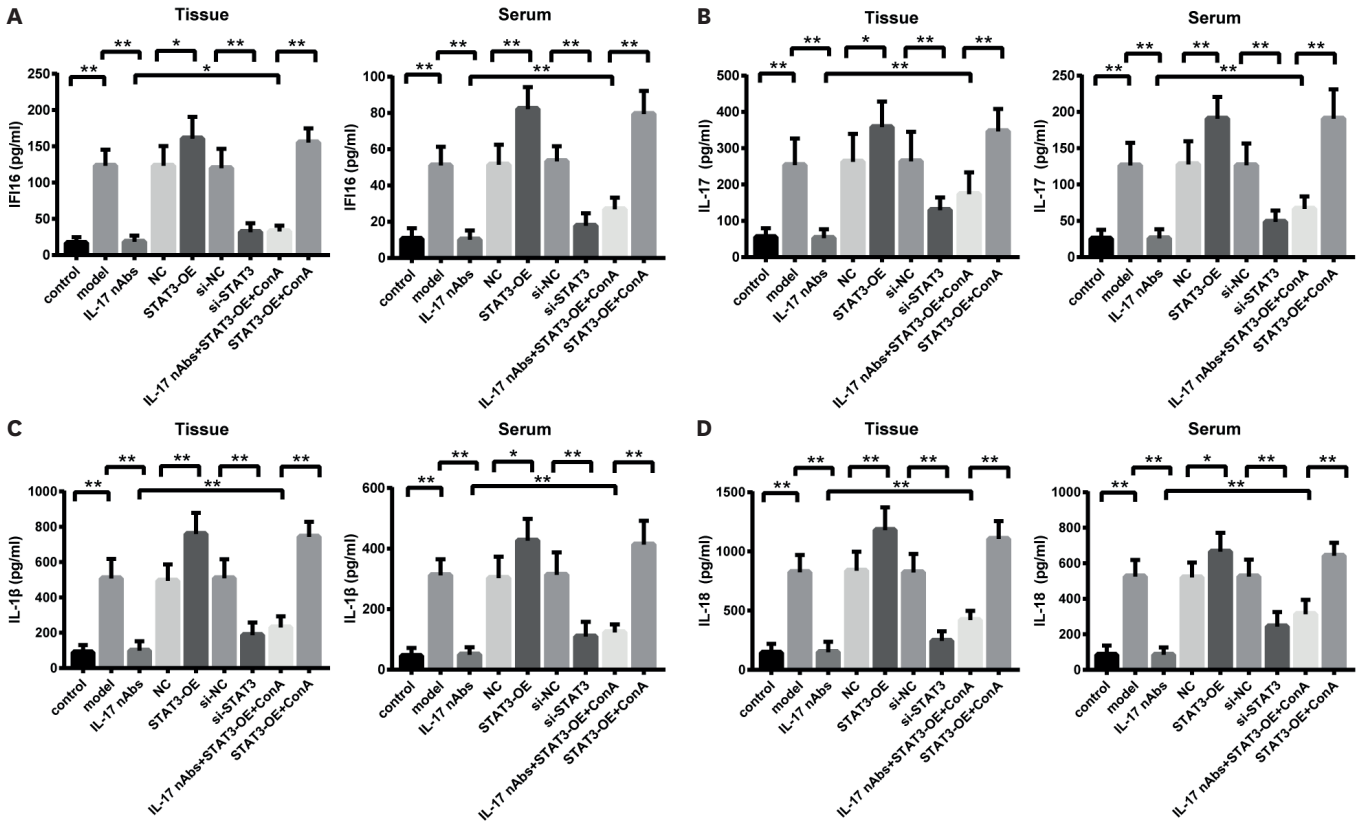

Figure 3. ELISA assay of in serum and liver from mice under different conditions. (A) IFI16, (B) IL-17, (C) IL-1β, (D) IL-18, (E) Comparison analysis between "IL-17 nAbs" group and "IL-17 nAbs+STAT3-OE+ConA" group.
Model (n=6), mice were challenged with ConA at a dosage of 15 mg/kg; NC (n=6), mice were challenged with ConA at a dosage of 15 mg/kg; Control (n=6), mice were received an equal amount of 0.9% normal saline; IL-17 nAbs (n=6), mice were administrated with IL-17 nAb (1 μg/kg) 24 h before were challenged with ConA at a dosage of 15 mg/kg; STAT3-OE (n=6), mice were given the short hairpin RNA lentivirus that up-regulated the expression of STAT3 at 10^8 virus per mouse every day for 7 days before were challenged with ConA at a dosage of 15 mg/kg; si-STAT3 (n=6), mice were given the short hairpin RNA lentivirus that down-regulated the expression at 10^8 virus per mouse every day for 7 days before were challenged with ConA at a dosage of 15 mg/kg; si-NC (n=6), mice were given the negative scrambled shRNA lentivirus that unregulated the expression at 10^8 virus per mouse every day for 7 days before were challenged with ConA at a dosage of 15 mg/kg; IL-17 nAbs+STAT3-OE+ConA (n=6), mice were administrated with IL-17 nAb (1 μg/kg) for 24 h, then were given the short hairpin RNA lentivirus that up-regulated the expression of STAT3 at 10^8 virus per mouse every day for 7 days before were challenged with ConA at a dosage of 15 mg/kg; STAT3-OE+ConA (n=6), mice were given the short hairpin RNA lentivirus that up-regulated the expression of STAT3 at 10^8 virus per mouse every day for 7 days before were challenged with ConA at a dosage of 15 mg/kg.
*p<0.05, **p<0.01.

ConA treatment (i.e. the model vs. control). There was no significant difference in pathology scores between model group or NC group and si-NC group. Although the pathology scores were additionally increased in mice treated with STAT3-OE lentivirus compared to that in NC group, there was no significant difference between these two groups (i.e. STAT3-OE vs. NC). The pathology scores were significantly decreased in mice treated with with si-STAT3 lentivirus compared to that in si-NC group injected with scrambled shRNA lentivirus ($p<0.01$, si-STAT3 vs. si-NC). Elevated pathology scores caused by ConA induced liver injury was significantly alleviated in mice administrated with IL-17 nAb compared to that in model group ($p<0.05$, IL-17 nAbs vs. model). In addition, the pathology scores were significantly decreased in mice treated sequentially with IL-17 nAb, STAT3-OE lentivirus and ConA compared to that in mice treated with STAT3-OE lentivirus and ConA (all $p<0.01$, IL-17 nAbs+STAT3-OE+ConA vs. STAT3-OE+ConA).

https://doi.org/10.4110/in.2023.23.e46

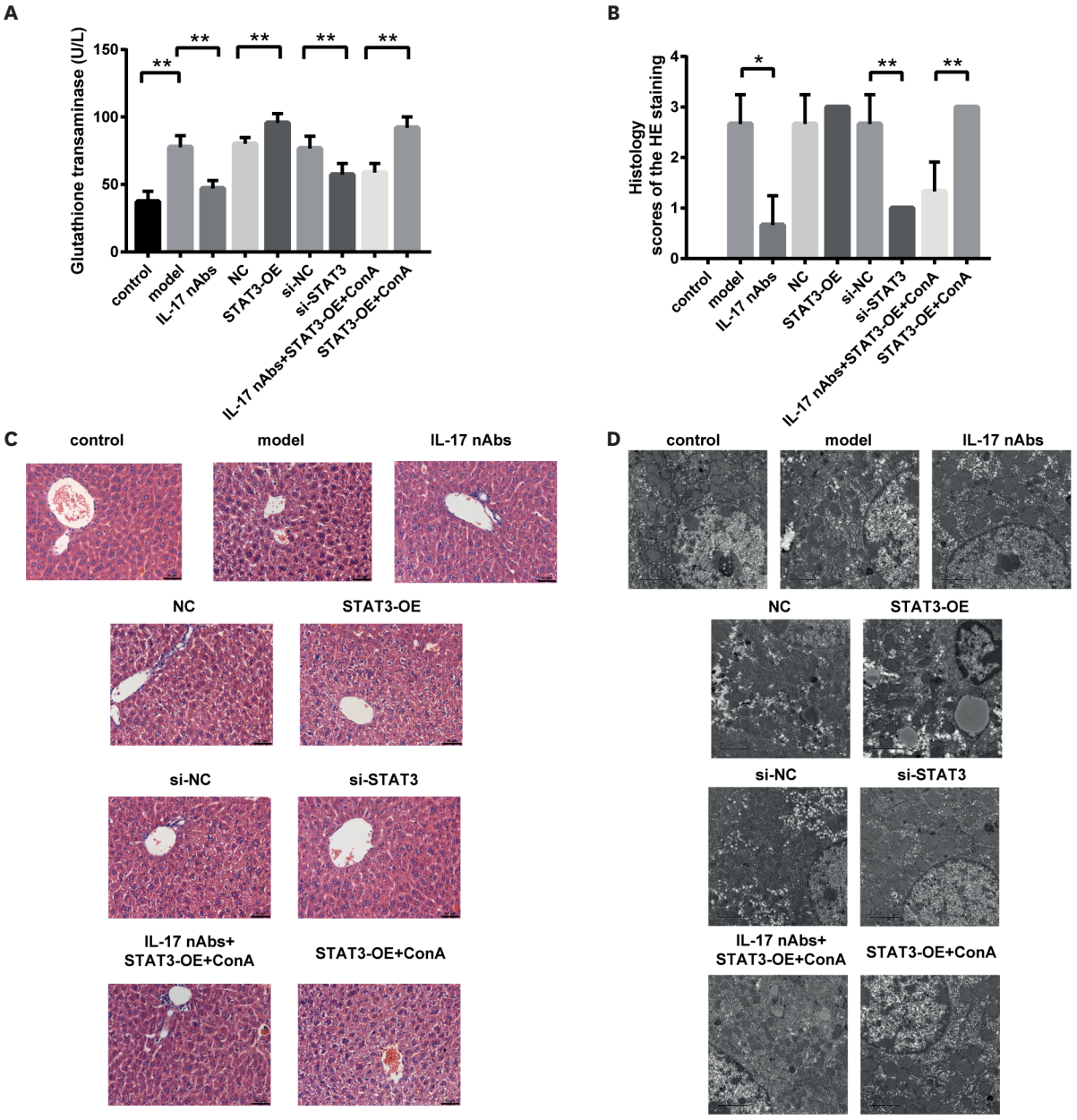

Figure 4. Pathological changes and damages in mice liver. (A) Glutathione transferase activity in serum from mice under different conditions. (B) The pathology scores on mice liver. (C) The histology changes in mice liver (H&E). (D) Observation of liver injury by TEM.
Model (n=6), mice were challenged with ConA at a dosage of 15 mg/kg; NC (n=6), mice were challenged with ConA at a dosage of 15 mg/kg; Control (n=6), mice were received an equal amount of 0.9% normal saline; IL-17 nAbs (n=6), mice were administrated with IL-17 nAb (1 μg/kg) 24 h before were challenged with ConA at a dosage of 15 mg/kg; STAT3-OE (n=6), mice were given the short hairpin RNA lentivirus that up-regulated the expression of STAT3 at 10^8 virus per mouse every day for 7 days before were challenged with ConA at a dosage of 15 mg/kg; si-STAT3 (n=6), mice were given the short hairpin RNA lentivirus that down-regulated the expression at 10^8 virus per mouse every day for 7 days before were challenged with ConA at a dosage of 15 mg/kg; si-NC (n=6), negative scrambled shRNA lentivirus that unregulated the expression of STAT was given at 10^8 virus per mouse every day for 7 days before were challenged with ConA at a dosage of 15 mg/kg; IL-17 nAbs+STAT3-OE+ConA (n=6), mice were administrated with IL-17 nAb (1 μg/kg) for 24 h, then were given the short hairpin RNA lentivirus that up-regulated the expression of STAT3 at 10^8 virus per mouse every day for 7 days before were challenged with ConA at a dosage of 15 mg/kg; STAT3-OE+ConA (n=6), mice were given the short hairpin RNA lentivirus that up-regulated the expression of STAT3 at 10^8 virus per mouse every day for 7 days before were challenged with ConA at a dosage of 15 mg/kg.
*p<0.05, **p<0.01.

https://doi.org/10.4110/in.2023.23.e46

Liver injury in mice treated with ConA, STAT3-OE lentivirus and IL-17 nAb

As demonstrated in **Fig. 4D**, TEM analysis showed that cytoplasmic looseness of hepatocytes, cystic dilatation of rough endoplasmic reticulum, and shedding of partial ribosomes from the surface of nuclear membrane appeared in the hepatic tissue from ConA induced AIH mice (i.e. model) compared to that in control group without ConA treatment (i.e. control). In addition, the degree of pathological damage of hepatocytes was aggravated in mice treated with STAT3-OE lentivirus (i.e. STAT3-OE). However, severity of pathological damage in liver was markedly reduced in mice treated with si-STAT3 lentivirus (i.e. si-STAT3) or IL-17 nAb (i.e. IL-17 nAbs and IL-17 nAbs+STAT3-OE+ConA).

DISCUSSION

IL-17 mediated immune response has been demonstrated to play a critical role in immune-mediated liver injury. It stimulates the activation of T lymphocytes and induces the differentiation of Th17 cells, resulting in immune cell infiltration, hepatic inflammation, and autoimmune hepatic disease (19-21). IL-17 promotes the release of proinflammatory cytokines such as IL-1β, IL-18, TNF-α and IFN-γ, and consequently activates the STAT3 pathway. STAT3 may interact with IFI16, which promoted the initiation of inflammation and linked to the pathogenesis of AIH. However, the role of IL-17 in AIH is still unclear, and there is a lack of comprehensive study on the mechanism of IL-17-STAT3-IFI16 axis in AIH. In the present study, we investigated the impact of IL-17-STAT3-IFI16 pathway on the pathogenesis of AIH using the primary hepatocytes model and BALB/c mouse model, respectively. AIH caused pathological damages with apparent pyroptosis morphology from the hepatocytes and mice liver were observed. Cell pyroptosis, known as cell inflammatory necrosis, is a novel programmed inflammatory cell death with a distinct cell morphology changes featured by constant cell expansion, membrane rupture, and release of proinflammatory cytokines. Various inflammatory cytokines released during pyroptosis might contribute to the activation of immunoresponse in infectious diseases such as AIH. It was found that the degree of liver injury can be alleviated, and the production of inflammation cytokines can be reduced by inhibiting the occurrence of IL-17 induced pyroptosis in inflammatory hepatic disease (25). Our study indicated that the levels of pyroptosis-related cytokines including IFI16, IL-1β and IL-18, together with GSDMD and cleaved caspase-1 were significantly changed in primary mouse hepatocytes, mice liver and serum after either adding IL-17 recombinant protein or IL-17 nAb to the cell culture or injecting IL-17 nAb to the mice. Especially, the levels of IFI16 were reduced in hepatocytes treated with IL-17 nAb, but IFI16 were significantly increased after further treatment with lentivirus up-regulated STAT3. This indicated that IFI16 induction is primarily driven by STAT3, thereby strengthening the evidence for the IL-17-STAT3-IFI16 axis. Further efforts should be made to investigate if there are other possible signaling pathways controlling IFI16 in elaborating the mechanisms behind AIH in future study. The TEM results showed that IL-17 recombinant protein promoted cell swelling with increased protrusion and vesicles, and deformed organelles. However, the degree of cell damage was alleviated in hepatocytes treated with IL-17 nAb. In addition, the histopathological damage of hepatocytes was aggravated in mice challenged with ConA compared to that in mice treated with IL-17 nAb before ConA injection. This further confirmed our finding that IL-17 may play an important role in promoting the pathological changes in AIH-related pyroptosis of hepatocytes.

The formation of inflammasomes is a key feature during pyroptosis, and IFI16 is an important component of inflammasomes. IFI16 is involved in progression of inflammation

processes. Several other studies has reported that the abnormal expression of IFI16 was found in autoimmune diseases (26,27). IL-17, IL-18, IL-1β and TNF-α may up-regulate the expression of IFI16, however the exact mechanism still remains unclear. Based on the preliminary results from dual-luciferase reporter assay, we found that there was certain binding interaction between STAT3 and IFI16 promoter region with consensus sequence of STAT3 and IFI16 (WT vs. Mut), and it may help to further explored the underlining mechanism of IFI16 in promoting AIH-related pyroptosis. However, the interaction between STAT3 and IFI16 needs to be further investigated through the CO-IP and GST-pull down experiments in future study. STAT3, as an important transcription factor, plays a critical role in autoimmune disease. Abnormal activation of STAT3 pathway has been confirmed in AIH (22). The results from our multiple assays indicated that the expression of IFI16 was increased in primary mouse hepatocytes treated with IL-17 recombinant protein, and was further elevated in hepatocytes treated with STAT3-OE lentivirus, whereas the expression of IFI16 was decrease in hepatocytes treated with si-STAT3 lentivirus. In addition, the cell morphology, levels of pyroptosis related effectors (IL-1β, IL-18, GSDMD cleaved caspase-1 and LDH) were significantly changed in cells treated with either STAT3-OE lentivirus or si-STAT3 lentivirus. Our results revealed that IL-17 may promote AIH-related pyroptosis through the STAT3-regulated expression of IFI16.

We employed the ConA-induced AIH mice for further evaluating the function of IL-17-STAT3-IFI16 axis in AIH-related pyroptosis. Our results showed that the expression levels of inflammatory cytokines (IFI16, IL-1β, IL-18, and IL-17) were significantly elevated, and the activity of serum glutathione transaminase was also significantly enhanced in ConA-induced AIH mice compared to that in control group. Consistently, the pathological injury was observed in liver tissue by H&E and TEM assays. We found that mice in STAT3-OE group showed even more aggravated liver damage compared to the mice in si-NC group, together with higher levels of inflammatory cytokines and increased activity of serum glutathione transaminase. Thus, our results indicated a promoted role of STAT3 on AIH-associated hepatocyte pyroptosis, and this was further illustrated in mice from si-STAT3 group with alleviated liver injury and reduced inflammatory cytokines and transferase activity. In addition, IL-17 nAb significantly reduced hepatocyte pyroptosis and alleviated histopathological changes in ConA-induced AIH in mice. Our data suggest that IL-17 played a critical role in IL-17-STAT3-IFI16 pathway, and contributed to the pathogenesis of hepatocyte pyroptosis in AIH disease. Other researchers have also reported that the inflammation-related hepatic injury can be alleviated by inhibiting IL-17 (21). In this light, IL-17 can be a potential therapeutic target for AIH disease.

Our study found that AIH-related pyroptosis was triggered by IL-17 mediated STAT3 activation and transcriptional regulation of IFI16. Thus, a better understanding of the IL-17-STAT3-IFI16 axis underlined the autoimmune attack to the liver cells in AIH-related pyroptosis may suggest new therapeutic strategies for AIH patients. In addition, Our preliminary results have demonstrated that the histological hepatic damages and serum aminotransferase levels were dramatically decreased in AIH mice administrated with IL-17 nAb. Thus, the development of novel treatments that target the IL-17-STAT3-IFI16 axis deserves to be further investigated for AIH disease.

In summary, our study revealed that IL-17 may play a key role in promoting the hepatocyte pyroptosis in AIH through regulating IFI16 by activated STAT3. The development of novel interventions targeting the IL-17-STAT3-IFI16 axis that worth to be further investigated.

ACKNOWLEDGEMENTS

This work was supported by grant from the Zhejiang Basic Public Welfare Research Project (LGF20H100001), founded by Zhejiang Provincial Department of Science and Technology.

REFERENCES

1. Siegel RL, Miller KD, Fuchs HE, Jemal A. Cancer statistics, 2022. *CA Cancer J Clin* 2022;72:7-33.
PUBMED | CROSSREF
2. Llovet JM, Kelley RK, Villanueva A, Singal AG, Pikarsky E, Roayaie S, Lencioni R, Koike K, Zucman-Rossi J, Finn RS. Hepatocellular carcinoma. *Nat Rev Dis Primers* 2021;7:6.
PUBMED | CROSSREF
3. Fujiwara N, Friedman SL, Goossens N, Hoshida Y. Risk factors and prevention of hepatocellular carcinoma in the era of precision medicine. *J Hepatol* 2018;68:526-549.
PUBMED | CROSSREF
4. Sharma R, Verna EC, Simon TG, Söderling J, Hagström H, Green PH, Ludvigsson JF. Cancer risk in patients with autoimmune hepatitis: a nationwide population-based cohort study with histopathology. *Am J Epidemiol* 2022;191:298-319.
PUBMED | CROSSREF
5. Doherty DG. Immunity, tolerance and autoimmunity in the liver: a comprehensive review. *J Autoimmun* 2016;66:60-75.
PUBMED | CROSSREF
6. Horst AK, Neumann K, Diehl L, Tiegs G. Modulation of liver tolerance by conventional and nonconventional antigen-presenting cells and regulatory immune cells. *Cell Mol Immunol* 2016;13:277-292.
PUBMED | CROSSREF
7. Dos Santos IP, de Assunção MT, Mauch RM, Sandy NS, Nolasco da Silva MT, Bellomo-Brandão MA, Riccetto AGL. Patients with treated autoimmune hepatitis and persistent suppression of plasmacytoid dendritic cells: a different point of view.
PUBMED | CROSSREF
8. Autoimmune hepatitis. *Nat Rev Dis Primers* 2018;4:18018.
PUBMED | CROSSREF
9. Rigopoulou EI, Dalekos GN. Current trends and characteristics of hepatocellular carcinoma in patients with autoimmune liver diseases. *Cancers (Basel)* 2021;13:102.
PUBMED | CROSSREF
10. Mack CL, Adams D, Assis DN, Kerkar N, Manns MP, Mayo MJ, Vierling JM, Alsawas M, Murad MH, Czaja AJ. Diagnosis and management of autoimmune hepatitis in adults and children: 2019 practice guidance and guidelines from the American Association for the Study of Liver Diseases. *Hepatology* 2020;72:671-722.
PUBMED | CROSSREF
11. European Association for the Study of the Liver. EASL clinical practice guidelines: autoimmune hepatitis. *J Hepatol* 2015;63:971-1004.
PUBMED | CROSSREF
12. Dalekos GN, Arvaniti P, Gatselis NK, Samakidou A, Gabeta S, Rigopoulou E, Koukoulis GK, Zachou K. First results from a propensity matching trial of mycophenolate mofetil vs. azathioprine in treatment-naive AIH patients. *Front Immunol* 2022;12:798602.
PUBMED | CROSSREF
13. Lohse AW, Sebode M, Jørgensen MH, Ytting H, Karlsen TH, Kelly D, Manns MP, Vesterhus M; European Reference Network on Hepatological Diseases (ERN RARE-LIVER); International Autoimmune Hepatitis Group (IAIHG). Second-line and third-line therapy for autoimmune hepatitis: a position statement from the European Reference Network on Hepatological Diseases and the International Autoimmune Hepatitis Group. *J Hepatol* 2020;73:1496-1506.
PUBMED | CROSSREF
14. Ikeda A, Aoki N, Kido M, Iwamoto S, Nishiura H, Maruoka R, Chiba T, Watanabe N. Progression of autoimmune hepatitis is mediated by IL-18-producing dendritic cells and hepatic CXCL9 expression in mice. *Hepatology* 2014;60:224-236.
PUBMED | CROSSREF
15. Zhao R, Zhou H, Su SB. A critical role for interleukin-1β in the progression of autoimmune diseases. *Int Immunopharmacol* 2013;17:658-669.
PUBMED | CROSSREF

16. Zhao L, Tang Y, You Z, Wang Q, Liang S, Han X, Qiu D, Wei J, Liu Y, Shen L, et al. Interleukin-17 contributes to the pathogenesis of autoimmune hepatitis through inducing hepatic interleukin-6 expression. *PLoS One* 2011;6:e18909.
PUBMED | CROSSREF
17. Nakayama S. Autoimmune hepatitis triggered by anti-TNF-α therapy. *Case Rep Med* 2013;2013:561748.
PUBMED | CROSSREF
18. Jaruga B, Hong F, Kim WH, Gao B. IFN-gamma/STAT1 acts as a proinflammatory signal in T cell-mediated hepatitis via induction of multiple chemokines and adhesion molecules: a critical role of IRF-1. *Am J Physiol Gastrointest Liver Physiol* 2004;287:G1044-G1052.
PUBMED | CROSSREF
19. Hammerich L, Heymann F, Tacke F. Role of IL-17 and Th17 cells in liver diseases. *Clin Dev Immunol* 2011;2011:345803.
PUBMED | CROSSREF
20. Singh B, Schwartz JA, Sandrock C, Bellemore SM, Nikoopour E. Modulation of autoimmune diseases by interleukin (IL)-17 producing regulatory T helper (Th17) cells. *Indian J Med Res* 2013;138:591-594.
PUBMED
21. Beringer A, Miossec P. IL-17 and IL-17-producing cells and liver diseases, with focus on autoimmune liver diseases. *Autoimmun Rev* 2018;17:1176-1185.
PUBMED | CROSSREF
22. Lorenzini T, Dotta L, Giacomelli M, Vairo D, Badolato R. STAT mutations as program switchers: turning primary immunodeficiencies into autoimmune diseases. *J Leukoc Biol* 2017;101:29-38.
PUBMED | CROSSREF
23. Yasumi Y, Takikawa Y, Endo R, Suzuki K. Interleukin-17 as a new marker of severity of acute hepatic injury. *Hepatol Res* 2007;37:248-254.
PUBMED | CROSSREF
24. Yu H, Huang J, Liu Y, Ai G, Yan W, Wang X, Ning Q. IL-17 contributes to autoimmune hepatitis. *J Huazhong Univ Sci Technolog Med Sci* 2010;30:443-446.
PUBMED | CROSSREF
25. Liu X, Zhang Z, Ruan J, Pan Y, Magupalli VG, Wu H, Lieberman J. Inflammasome-activated gasdermin D causes pyroptosis by forming membrane pores. *Nature* 2016;535:153-158.
PUBMED | CROSSREF
26. Lei L, Sun J, Han J, Jiang X, Wang Z, Chen L. Interleukin-17 induces pyroptosis in osteoblasts through the NLRP3 inflammasome pathway in vitro. *Int Immunopharmacol* 2021;96:107781.
PUBMED | CROSSREF
27. Caneparo V, Cena T, De Andrea M, Dell'oste V, Stratta P, Quaglia M, Tincani A, Andreoli L, Ceffa S, Taraborelli M, et al. Anti-IFI16 antibodies and their relation to disease characteristics in systemic lupus erythematosus. *Lupus* 2013;22:607-613.
PUBMED | CROSSREF
28. De Andrea M, De Santis M, Caneparo V, Generali E, Sirotti S, Isailovic N, Guidelli GM, Ceribelli A, Fabbroni M, Simpatico A, et al. Serum IFI16 and anti-IFI16 antibodies in psoriatic arthritis. *Clin Exp Immunol* 2020;199:88-96.
PUBMED | CROSSREF
29. Matsuda T, Muromoto R, Sekine Y, Togi S, Kitai Y, Kon S, Oritani K. Signal transducer and activator of transcription 3 regulation by novel binding partners. *World J Biol Chem* 2015;6:324-332.
PUBMED | CROSSREF